Organic Process Research & Development **2003**, *7*, 202−208

Technology Reports

Synthesis of *p*-Aminophenol by Catalytic Hydrogenation of *p*-Nitrophenol

Manisha J. Vaidya, Shrikant M. Kulkarni, and Raghunath V. Chaudhari*

Homogeneous Catalysis Division, National Chemical Laboratory, Pune - 411 008, India

Abstract:

The catalytic hydrogenation of *p*-nitrophenol to *p*-aminophenol was investigated in a laboratory-scale batch-slurry reactor. Pt/C catalyst (1%) was chosen for optimization of reaction conditions and kinetic studies because of its higher catalytic activity compared to that of other heterogeneous transition metal catalysts. The average catalytic activity and initial rate of hydrogenation was found to increase with increase in the solvent polarity. To investigate the intrinsic kinetics of the reaction, the effect of catalyst loading, agitation speed, *p*-nitrophenol concentration, and hydrogen partial pressure on the initial rate of hydrogenation was studied at different temperatures. The analysis of initial rate data indicated that the mass-transfer resistances were not significant under the prevailing reaction conditions. A simple Langmuir−Hinschelwood (L−H)-type model was found to represent the kinetics of hydrogenation of *p*-nitrophenol to *p*-aminophenol satisfactorily. The apparent energy of activation was found to be 61 kJ/mol.

Introduction

p-Aminophenol is an important intermediate in the preparation of several analgesic and antipyretic drugs such as paracetamol, acetanilide, phenacetin, and so forth.[1] It is a strong reducing agent and is used as a photographic developer. It is also used as a corrosion inhibitor in paints and anticorrosion-lubricating agent in fuels for two-cycle engines. In the dye industry, *p*-aminophenol is used as a wood stain, imparting a roselike color to timber, and as a dyeing agent for fur and feathers.[1] A major process for the preparation of *p*-aminophenol is via the hydrogenation of nitrobenzene in the presence of strong acids such as sulfuric acid. The initial hydrogenation of nitrobenzene leads to the formation of intermediate phenylhydroxylamine, which rearranges to *p*-aminophenol in the presence of acid (Bamberger rearrangement). Conventionally, the conversion of nitrobenzene to *p*-aminophenol has been carried out using a stoichiometric amount of iron−acid reducing agent. The major drawback of this process is the formation of an almost equivalent amount of Fe−FeO sludge, which cannot be reused and causes severe disposal problems.[2] The transition metal-catalyzed hydrogenation of nitrobenzene to *p*-aminophenol in the presence of aqueous acid obviates the sludge-formation problem.[3] However, the nitrobenzene hydrogenation route for *p*-aminophenol, either conventional or catalytic, has two major drawbacks: (1) the quantitative formation of side products such as aniline via further hydrogenation of the intermediate phenylhydroxylamine, and (2) the use of highly corrosive mineral acid. In view of the growing demands for *p*-aminophenol, there exists a scope for the exploration of other efficient and greener catalytic routes.

Scheme 1. **Catalytic hydrogenation of *p*-nitrophenol to *p*-aminophenol**

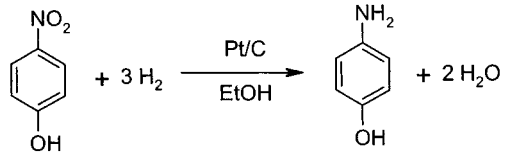

The direct catalytic hydrogenation of *p*-nitrophenol could be an attractive route for the preparation of *p*-aminophenol (Scheme 1). The starting material for this route can be obtained either by nitration of phenol or hydrolysis of *p*-nitrochlorobenzene. Apart from the conventional Fe−acid reduction route,[4] several heterogeneous transition metal catalysts containing Pd, Pt, Ni, Rh, and so forth have been reported for this reaction in previous literature.[5]

However, the available information on the catalytic hydrogenation of *p*-nitrophenol to *p*-aminophenol is rather qualitative in nature, and there is no report on the systematic study of the effect of various reaction parameters and intrinsic reaction kinetics. Yao et al.[6] investigated the liquid-phase hydrogenation of *p*-nitrophenol using colloidal Pd, Pt, Rh, and Raney Ni catalysts and proposed an empirical rate equation for the hydrogenation rate. In the only significant report, Malpani et al.[7] investigated the preliminary kinetics of hydrogenation of *p*-nitrophenol to *p*-aminophenol using 1% Pd/C catalyst in ethanol solvent. In view of the commercial importance of *p*-aminophenol, the primary objective of this work was to first identify a suitable

* To whom correspondence should be addressed. Fax: (+91) 20 5893260. E-mail: rvc@ems.ncl.res.in.

(1) Mitchell, S. *Kirk-Othmer Encyclopedia of Chemical Technology*, 4th ed.; Wiley-Interscience: New York, 1992; Vol. II, p 580.
(2) Rode, C.; Vaidya, M.; Chaudhari, R. *Org. Process Res. Dev.* **1999**, *3*, 465.
(3) Caskey, C.; Chapman, D. U.S. Patent 4,571,437, 1986.
(4) (a) Skipka, G.; Alles, H.; Duerholz, F.; Lidner, O. DE 2930754, 1981. (b) Shah, J.; Mahajan, S. *Chem. Ind. Dev. Ann.* **1977**, *C*, 19.
(5) (a) Siddheshwaran, P.; Hrishnan, V.; Bhat, A. *Ind. J. Chem.* **1997**, *36*, 149. (b) Freifelder, M.; Robinson, R. U.S. Patent 3,079,435, 1963.
(6) (a) Yao, H.; Emmett, P. *J. Am. Chem. Soc.* **1959**, *81*, 4125. (b) Yao, H.; Emmett, P. *J. Am. Chem. Soc.* **1961**, *83*, 796. (c) Yao, H.; Emmett, P. *J. Am. Chem. Soc.* **1962**, *84*, 1086.
(7) Malpani, P.; Chandalia, S. *Ind. Chem. J.* **1973**, 15.

Published on Web 01/24/2003
10.1021/op025589w CCC: $25.00

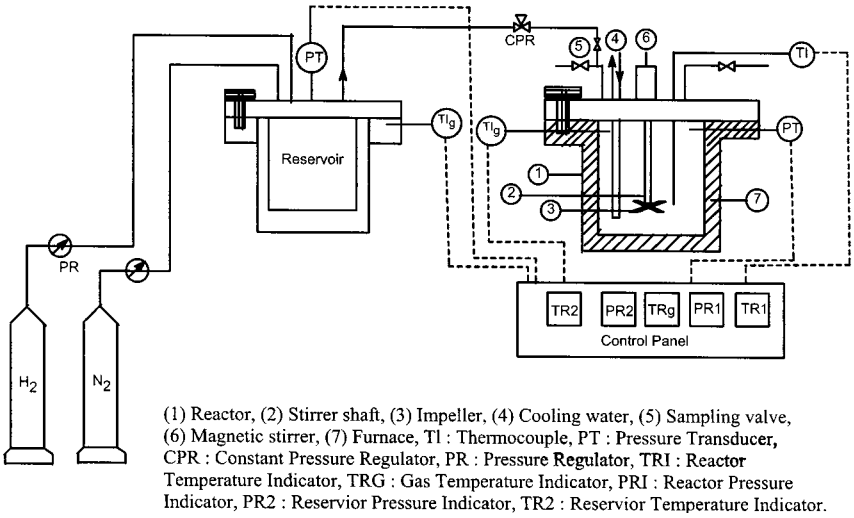

Figure 1. **Schematic of the reactor setup used for hydrogenation experiments.**

heterogeneous catalyst for the efficient hydrogenation of *p*-nitrophenol to *p*-aminophenol. The second objective was to investigate the intrinsic kinetics of this reaction using a suitable catalyst with detailed analysis of mass-transfer effects and to further develop rate equations that could be useful for design applications.

Experimental Section

Materials. *p*-Nitrophenol, ethanol, and other solvents were purchased from SD Fine Chemicals, Mumbai (India). The water content in ethanol was 10% as determined using Karl Fischer method. Hydrogen gas was purchased from Industrial Oxygen Limited, Pune (India) and directly used from cylinder. The purities of hydrogen and nitrogen gases were greater than 99.5%. The catalysts (1% Pt/C, 1% Pd/C, 1% Ru/C, 1% Rh/C, 1% Pt/Al_2O_3, 3% Pt/C) and *p*-aminophenol were purchased from Aldrich Chemicals (U.S.A.). Other supported catalysts were prepared using standard literature procedures.

Experimental Setup. The hydrogenation experiments were carried out in a 50-mL capacity stainless steel autoclave (Parr Instruments Company, U.S.A.) fitted with a magnetically driven impeller with a four-blade stirrer capable of operations up to 1500 rpm. The temperature of the liquid in the reactor was maintained at a desired value (±1 K) with the help of a PID controller, which provided an alternate heating and cooling arrangement. The reactor was also equipped with an internal thermocouple and a digital pressure transducer (with the precision of ±1 psig) for temperature and pressure monitoring, respectively. The relevant safety features such as a rupture disk and a high temperature−pressure cutoff were also installed as a part of the reactor setup. The schematic of the reactor setup is shown in Figure 1.

Experimental Procedure. In a typical hydrogenation experiment, predetermined quantities of *p*-nitrophenol, catalyst, and solvent were charged into a clean autoclave. The autoclave was then closed, and the contents were flushed first with nitrogen and then with hydrogen. The reactor was then heated to a desired temperature under slow stirring (100 rpm). After the temperature equilibrated at the set point, hydrogen gas was introduced into the reactor to a predetermined level, and the contents were stirred vigorously (1000 rpm). A constant pressure was maintained throughout the reaction course by supplying hydrogen from a reservoir vessel through a constant pressure-regulator valve. The pressure drop in the reservoir vessel was measured as a function of time. After the expected amount of hydrogen was consumed, the reactor was cooled to room temperature, and the excess hydrogen was vented off. The reaction mixture was further diluted by acetonitrile and analyzed by gas chromatography for *p*-nitrophenol and *p*-aminophenol content.

Analytical Methods

The analysis of all liquid samples was carried out using a Hewlett-Packard gas chromatograph (model HP 6890). The analysis conditions were the following:

(1) column: HP-1 capillary column (30 m × 0.32 mm)
(2) oven temperature: 433 K
(3) injection temperature: 523 K
(4) detector (FID) temperature: 523 K
(5) carrier gas nitrogen (flow rate: 30 mL/min). Calibration factors were determined by analyzing liquid standards having known compositions of *p*-nitrophenol and *p*-aminophenol. The quantitative analytical procedure was found to have a relative error of 2−4%.

Results and Discussion

A. Catalyst Selection. The hydrogenation of *p*-nitrophenol to *p*-aminophenol (Scheme 1) was investigated in a laboratory-scale batch-slurry reactor in which the concentration−time and hydrogen consumption data were obtained. To compare the activity performance of various catalysts for the hydrogenation reaction, the experimental results were expressed in terms of initial rate of hydrogenation and average catalytic activity. The initial rate of hydrogenation (R_A) was calculated from the hydrogen consumption−time data essentially under low-conversion conditions (<10−20%). The average catalytic activity (N) expressed as kmol/kg·h, was defined as the amount of

Table 1. **Initial rate of hydrogenation and average catalytic activity for various heterogeneous catalysts[a]**

sr.	catalyst	$R_A \times 10^3$ (kmol/m^3·s)	N (kmol/kg·h)
1	1% Pd/C	0.501	0.595
2	1% Ni/C	0.199	0.446
3	1% Rh/C	0.166	0.380
4	1% Ru/C	0.016	0.034
5	1% Pt/C	1.096	1.960
6	1% Pt/Al_2O_3	0.333	0.812
7	1% Pt/SiO_2	0.109	0.185
8	1% Pt/HY	0.082	0.131
9	0.5% Pt/C	0.524	1.347
10	2% Pt/C	2.034	2.412
11	3% Pt/C	2.895	3.017

[a] Reaction conditions: *p*-nitrophenol, 0.479 kmol/m^3; catalyst, 0.266 kg/m^3; ethanol, 30 × 10^{-6} m^3; hydrogen pressure, 2.72 MPa; temperature, 353 K; agitation speed, 1000 rpm.

Table 2. **Effect of solvent on the rate of hydrogenation and average catalytic activity[a]**

sr.	solvent	(ϵ)	$R_A \times 10^3$ (kmol/m^3·s)	N (kmol/kg·h)
1	water	78.5	1.325	3.066
2	methanol	32.6	1.170	2.160
3	ethanol	24.3	1.096	1.960
4	*n*-propanol	20.1	0.776	1.790
5	*n*-butanol	17.8	0.406	0.342

[a] Reaction conditions: *p*-nitrophenol, 0.479 kmol/m^3; catalyst (1% Pt/C), 0.266 kg/m^3; solvent, 30 × 10^{-6} m^3; hydrogen pressure, 2.72 MPa; temperature, 353 K; agitation speed, 1000 rpm. The values of dielectric constant (ϵ) were taken from CRC Handbook.[9]

p-nitrophenol consumed per unit weight of the catalyst per hour, based on the time required to achieve more than 99% conversion of *p*-nitrophenol.

The activities of several heterogeneous transition metal catalysts were investigated for the hydrogenation of *p*-nitrophenol to *p*-aminophenol, and the results are presented in Table 1. The initial rate of hydrogenation and the average catalytic activity followed the order Pt > Pd > Ni > Rh > Ru. Thus, the highest catalytic activity and hydrogenation rate was observed for platinum catalyst (1% Pt/C), whereas ruthenium catalyst had the least activity (only 10% conversion in 5 h). The effect of catalyst support on the catalyst activity was also investigated (Table 1, entries 5−8). It was observed that the carbon-supported platinum catalyst had the highest activity. Therefore, further experiments were carried out using platinum-on-carbon catalyst. The initial rate of hydrogenation as well as the average catalytic activity increased with the platinum content in the catalyst (Table 1, entries 5, 9−11).

The effect of various solvents on the initial rate of hydrogenation and catalytic activity was also investigated briefly, and the results are presented in Table 2. The solvents used for this study included water, methanol, ethanol, *n*-propanol, and *n*-butanol. It was observed that the average catalytic activity and the initial rate of hydrogenation increased with increase in the solvent polarity and were highest in water. Such enhancement in the reaction rates with increase in the solvent polarity has been previously observed

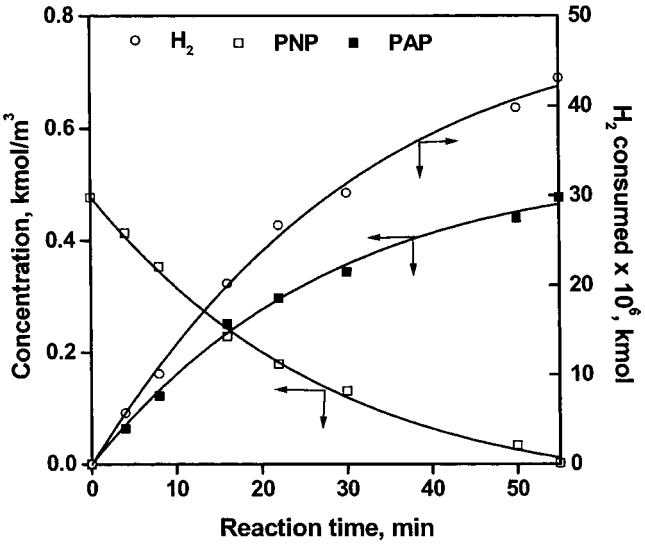

Figure 2. **Typical concentration−time profile for hydrogenation of *p*-nitrophenol. Reaction conditions: *p*-nitrophenol, 0.479 kmol/m^3; catalyst (1% Pt/C), 0.266 kg/m^3; ethanol, 30 × 10^{-6} m^3; hydrogen pressure, 2.72 MPa; temperature, 353 K; agitation speed, 1000 rpm.**

Table 3. **Range of operating conditions for kinetic studies**

1	temperature	308−353 K
2	hydrogen pressure	1.36−6.80 MPa
3	catalyst loading	0.133−0.399 kg/m^3
4	*p*-nitrophenol concentration	0.119−0.958 kmol/m^3
5	agitation speed	600−1200 rpm

for hydrogenation of nitro compounds by Rajadhyaksha et al.[8] and was partly attributed to the increase in activity of nitro compounds in polar solvents. Despite the highest catalytic activity in water, we preferred ethanol as solvent for further studies because of higher solubility of *p*-nitrophenol and *p*-aminophenol in ethanol compared to that in water.

B. Kinetic Studies. The preliminary experiments on the hydrogenation of *p*-nitrophenol using 1% Pt/C catalyst showed that the material balance, when based on the molar amount of liquid-phase reactants (*p*-nitrophenol and hydrogen) consumed and the molar amount of the product (*p*-aminophenol) formed were consistent with the stoichiometric reaction given in Scheme 1 within 96−99% in all experiments. The typical concentration−time profile at 353 K is shown in Figure 2. No side products were detected in the range of conditions studied. Also, no hydrogenation was found to occur in the absence of the catalyst, which confirmed the absence of any noncatalytic reaction. Therefore, for all kinetic experiments, the change in hydrogen pressure in the reservoir vessel with time was observed under different reaction conditions. The activity of the catalyst remained relatively unchanged even after repeated use (four times), which indicated the constancy of catalytic activity during a kinetic experiment. Several experiments were carried out over a reasonably wide range of operating conditions, which are summarized in Table 3.

(8) Rajadhyaksha, R.; Karwa, S. *Chem. Eng. Sci.* **1986**, *41*, 1765.

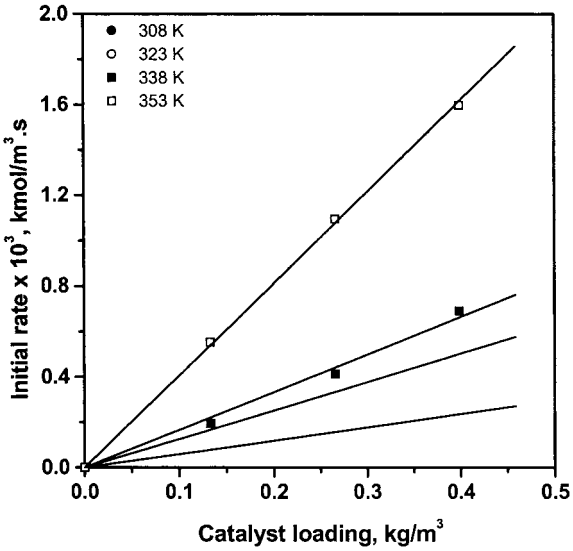

Figure 3. **Effect of catalyst loading on the initial rate of hydrogenation. Reaction conditions: *p*-nitrophenol, 0.479 kmol/m^3; ethanol, 30 × 10^{-6} m^3; hydrogen pressure, 2.72 MPa; agitation speed, 1000 rpm.**

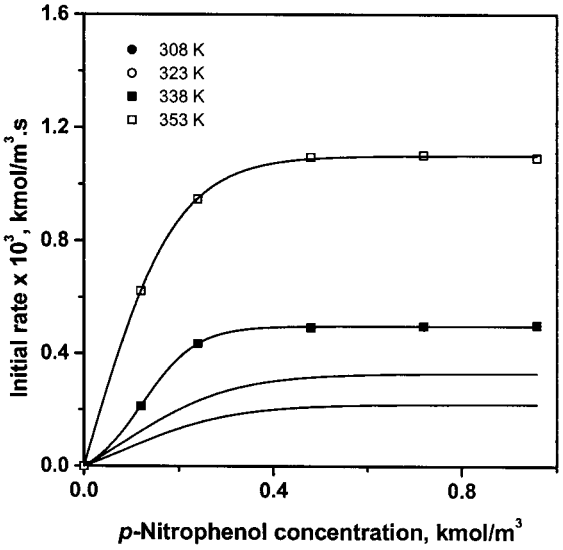

Figure 5. **Effect of *p*-nitrophenol concentration on the initial rate of hydrogenation. Reaction conditions: catalyst (1% Pt/C), 0.266 kg/m^3; ethanol, 30 × 10^{-6} m^3; hydrogen pressure, 2.72 MPa; agitation speed, 1000 rpm.**

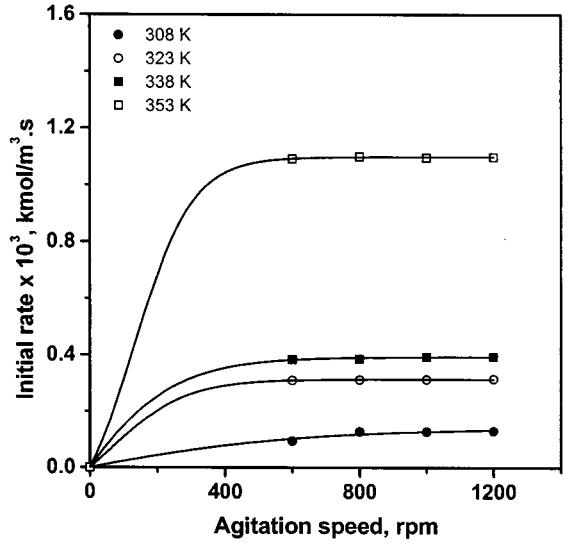

Figure 4. **Effect of agitation speed on the initial rate of hydrogenation. Reaction conditions: *p*-nitrophenol, 0.479 kmol/m^3; catalyst (1% Pt/C), 0.266 kg/m^3; ethanol, 30 × 10^{-6} m^3; hydrogen pressure, 2.72 MPa.**

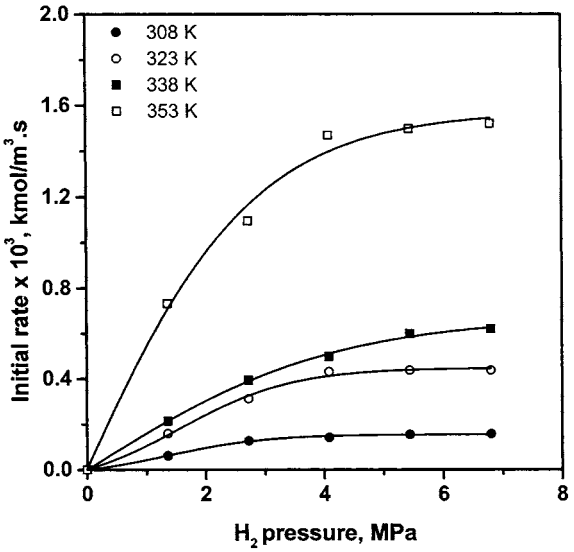

Figure 6. **Effect of hydrogen pressure on the initial rate of hydrogenation. Reaction conditions: *p*-nitrophenol, 0.479 kmol/m^3; catalyst (1% Pt/C), 0.266 kg/m^3; ethanol, 30 × 10^{-6} m^3; agitation speed, 1000 rpm.**

C. Analysis of Initial Rate Data. The analysis of initial rate data provides a first approach to understand the dependency of reaction rates on the individual parameters and also in the evaluation of the significance of mass-transfer effects. Therefore, the effect of catalyst loading, agitation speed, *p*-nitrophenol concentration, and hydrogen partial pressure on the initial rate of hydrogenation was investigated, and the results are presented in Figures 3−6. The initial rate of hydrogenation varied linearly with respect to catalyst loading (Figure 3) and had a zero intercept, suggesting that the gas−liquid mass-transfer resistance may not be significant. This conclusion was further supported by the effect of agitation speed on the hydrogenation rate (Figure 4). The initial rate of hydrogenation was independent of agitation speed above 600 rpm, confirming the kinetic regime. Further kinetic experiments were therefore conducted at an agitation speed of 1000 rpm. The effect of *p*-nitrophenol concentration on the initial rate of hydrogenation (Figure 5) showed zero-order dependence except at lower concentrations (less than 0.4 kmol/m^3). The effect of hydrogen partial pressure on the initial rate of hydrogenation was investigated in the range of 1.36−6.80 MPa, and the results are shown in Figure 6. The hydrogenation rate increased with increase in the hydrogen pressure until 4.08 MPa and thereafter remained almost unaffected. The general trend of zero-order dependence of hydrogenation rate with respect to nitro aromatics[10] and a fractional order with respect to hydrogen[11] is consistent

(9) Weast, R., Ed. *Handbook of Chemistry and Physics*, 53rd ed.; The Chemical Rubber Co.: Cleveland, Ohio, 1973.
(10) Rode, C.; Chaudhari, R. *Ind. Eng. Chem. Res.* **1994**, *33*, 1645.

with previous reports on hydrogenation of other nitro aromatics.

D. Analysis of Mass-Transfer Effects. The catalytic hydrogenation of *p*-nitrophenol is an example of a multiphase catalytic reaction, and therefore, it was important to ensure that the mass-transfer and hydrodynamic factors were eliminated or accounted for when determining the intrinsic reaction kinetics. For a typical gas−liquid−solid reaction, like the present one, various mass-transfer resistances such as gas−liquid, liquid−solid, and intraparticle diffusion are likely to exist. The effect of catalyst loading and the agitation speed on the initial rate of hydrogenation suggested the absence of gas−liquid mass transfer under the prevailing reaction conditions. To analyze the contribution of different mass-transfer steps, quantitative criteria suggested by Ramchandran and Chaudhari[12] were also used, which for the absence of mass-transfer effects are:

Gas−Liquid Mass Transfer

$$\alpha_1 = \frac{R_A}{k_L a_B A^*} < 0.1 \tag{1}$$

Liquid−Solid Mass Transfer

$$\alpha_2 = \frac{R_A}{k_S a_P A^*} < 0.1 \tag{2}$$

Intraparticle Diffusion

$$\phi_{exp} = \frac{d_P}{6}\left[\frac{\rho_P R_A}{w D_{eA} A^*}\right]^{0.5} < 0.2 \tag{3}$$

The factors α_1, α_2, and ϕ_{exp} which represent the ratios of the observed rate of reaction to the maximum possible rate of gas−liquid, liquid−solid, and intraparticle mass-transfer rates, respectively, were evaluated from the initial rate data for all temperatures. The values of gas−liquid (k_La) and liquid−solid (k_S) mass-transfer coefficients and diffusivity of hydrogen required in eqs 1−3 were estimated using the correlations described by Chaudhari et al.,[13] Sano et al.,[14] and Wilke and Chang,[15] respectively. The tortuosity and porosity of the catalyst were assumed to be 3 and 0.6, respectively.[16] The value of particle diameter used in the calculation of intraparticle diffusion was 10 μm. The solubility of hydrogen in 90% ethanol was measured experimentally using absorption technique (Table 4). Since the calculated values of α_1, α_2, and ϕ_{exp} were less than 0.1, 0.1, and 0.2 respectively for all the rate data, the gas−liquid, liquid−solid, and intraparticle diffusion resistances were assumed to be negligible.

Table 4. **Henry's constant for hydrogen in 90% ethanol at different temperatures**

temperature (K)	$H \times 10^2$ (kmol/m^3·MPa)
308	3.399
323	3.511
338	3.624
353	3.734

E. Rate Equations and Kinetic Parameters. The observed rate data were fitted to several forms of rate equations. Rate equations corresponding to models I and II were purely empirical, whereas that corresponding to model III was derived by assuming that the species A and B (hydrogen and *p*-nitrophenol, respectively) compete for the single-site adsorption. The list of rate equations and the corresponding final optimized model parameters are given in Table 5.

The indicated model parameters were evaluated by a nonlinear regression analysis using an optimization routine based on the Marquardt's method.[17] For this purpose, the objective function was chosen as follows

$$\psi = \sum_{i=1}^{q} (r_{exp} - r_{mod})_i^2 \tag{4}$$

The nonlinear regression analysis was performed to estimate the kinetic parameters such that the objective function ψ has minimum value. Since the magnitude of the ψ value for all models was more or less in the same range, further model discrimination was performed on the basis of physicochemical constraints. It should be noted that since the estimation of kinetic parameters is done purely on the mathematical basis, they do not account for any thermodynamic significance. According to the physicochemical constraints, the kinetic parameters have to satisfy a few conditions derived from the thermodynamic considerations as summarized below.[18−20]

Rule 1. $k > 0$ (k should be positive)

Rule 2. $E_a > 0$ (the energy of activation should be positive)

Although, all the three models satisfied the above criteria, a closer look at Table 5 reveals that the kinetic parameters for models I and III do not follow any general trend (either decreasing or increasing) with temperature and therefore can be rejected leaving only model II. Although the value of adsorption equilibrium constants for model II increases with increase in temperature, which is contrary to the normal observation, it must be noted that these constants were evaluated by mathematically fitting the experimental data to a model, and therefore, these values should be considered as empirical constants. Such an observation, although rare, has been reported previously.[21] The apparent energy of activation and heats of adsorption for hydrogen and *p*-

(11) Rajshekharam, M.; Nikalje, D.; Jaganathan, R.; Chaudhari, R. *Ind. Eng. Chem. Res*. **1997**, *36*, 592.
(12) Ramchandran, P.; Chaudhari, R. *Three Phase Catalytic Reactors*; Gordon and Breach Science Publishers: New York, 1983.
(13) Chaudhari, R.; Gholap, R.; Emig, G.; Hofmann, H. *Can. J. Chem. Eng.* **1987**, *65*, 744.
(14) Sano, Y.; Yamaguchi, N.; Adachi, T. *J. Chem. Eng. Jpn.* **1974**, *1*, 255.
(15) Wilke, C.; Chang, P. *AIChE J.* **1955**, *1*, 264.
(16) (a) Satterfield, C. *Mass Transfer in Heterogeneous Catalysis*; MIT Press: Cambridge, MA, 1970. (b) Komiyama, H.; Smith, J. *AIChE J*. **1975**, *21*, 670.
(17) Marquardt, D. *J. Soc. Ind. Appl. Math.* **1963**, *11*, 431.
(18) Boudart, M. *AIChE J.* **1972**, *18*, 465.
(19) Vennice, M.; Hyun, S.; Kalpackici, B.; Liauh, W. *J. Catal.* **1979**, *56*, 358.
(20) Kapteyn, F. Ph.D. Dissertation, University of Amsterdam, Amsterdam, The Netherlands, 1986.

Table 5. **Rate equations and kinetic parameters**

model	rate equation[a]	temperature (K)	k_1 (m^3/kg)(m^3/kmol·s)	K_A (m^3/kmol)	K_B (m^3/kmol)(m^3/kmol)	$\Psi_{min} \times 10^9$
I	$R_A = wk_1AB/(1 + K_AA)(1 + K_BB)$	308	2.026×10^{-2}	5.741	4.262	2.367
		323	3.086×10^{-2}	6.232	4.394	6.970
		338	4.501×10^{-2}	4.487	6.166	1.250
		353	17.090×10^{-2}	7.249	7.476	51.17
II	$R_A = wk_1AB/(1 + K_AA + K_BB)$	308	3.090	2.606×10^3	9.837×10^2	2.385
		323	4.842	2.843×10^3	1.077×10^3	7.374
		338	14.774	5.453×10^3	2.824×10^3	1.763
		353	64.484	1.029×10^4	4.321×10^3	100.8
III	$R_A = wk_1AB/(1 + K_AA + K_BB)^2$	308	1.927×10^{-2}	3.890	1.489	1.625
		323	3.048×10^{-2}	4.166	1.623	4.339
		338	3.771×10^{-2}	3.396	1.704	2.106
		353	15.880×10^{-2}	5.529	2.300	2.824

[a] A: liquid-phase concentration of hydrogen, kmol/m^3; B: liquid-phase concentration of *p*-nitrophenol, kmol/m^3.

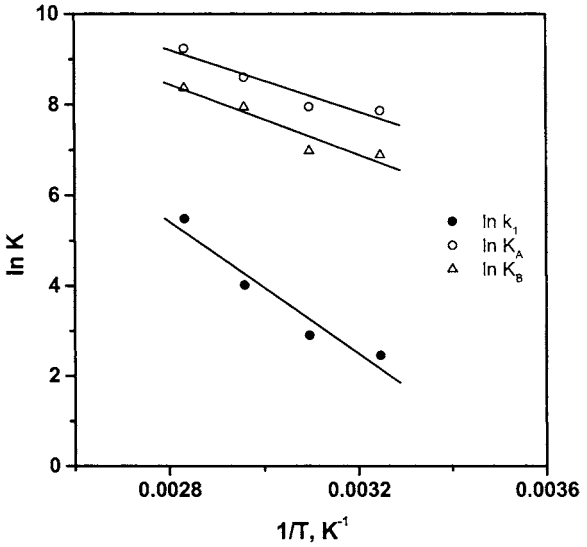

Figure 7. **Temperature dependence of kinetic rate and adsorption equilibrium parameters for model II.**

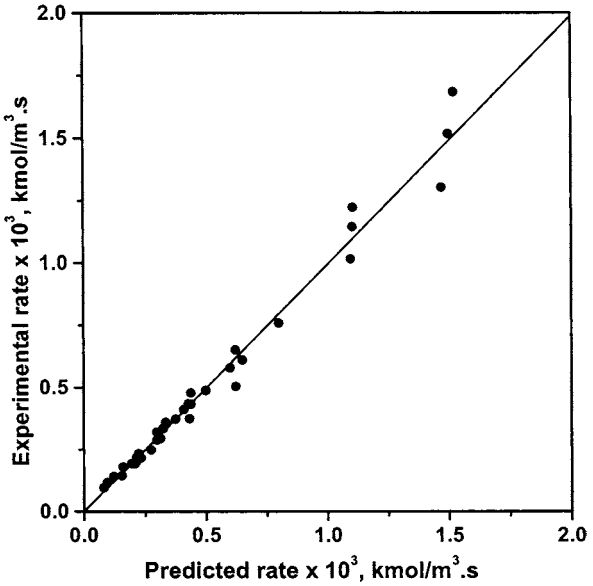

Figure 8. **Comparison of experimental and predicted hydrogenation rates.**

nitrophenol as calculated using the Arrhenius equation (Figure 7) for model II was 60.98, 28.40, and 32.31 kJ/mol, respectively. The standard deviation in fitting the ln *k* curves for k_1, K_A, and K_B was 0.43, 0.24, and 0.27, respectively.

To assess the adequacy of the rate model II and the accuracy of the kinetic parameters, the results of the fittings were also analyzed using the statistical criteria suggested by Kitrell[22] and Froment and Bischoff.[23] Thus, the results obtained using model II were subjected for the residual analysis in which a relative residuals (RR) defined as

$$RR = \frac{r_{exp} - r_{mod}}{r_{exp}} \quad (5)$$

were plotted as a function of hydrogen partial pressure and *p*-nitrophenol concentration. It was observed that the relative residuals were distributed with almost zero means and exhibited no trend as a function of any independent variable. A further comparison of the experimental and predicted rate data (using model II) is shown in Figure 8. In view of the excellent agreement between the experimental and predicted rate values, it could be concluded that model II satisfactorily represents the intrinsic kinetics of the hydrogenation of *p*-nitrophenol to *p*-aminophenol using 1% Pt/C catalyst. Also, the results obtained using this model satisfy the thermodynamic as well as the statistical constraints.

Conclusions

The hydrogenation of *p*-nitrophenol to *p*-aminophenol was investigated in a laboratory-scale batch-slurry reactor. Pt/C (1% (w/w)) was identified as a suitable catalyst among the several heterogeneous transition metal catalysts because its catalyst activity is the greatest. A brief investigation on the effect of solvent on the hydrogenation rate and average catalytic activity was also carried out. The hydrogenation rate as well as the catalytic activity was found to increase with an increase in the solvent polarity. The effect of catalyst loading, agitation speed, hydrogen pressures, and initial

(21) (a) Chaudhari, R.; Parande, M.; Ramchandran, P.; Brahme, P.; Vadgaonkar, H.; Jaganathan, R. *AIChE J.* **1985**, *31*, 1891. (b) Broderick, D.; Gates, B. *AIChE J.* **1981**, *27*, 663.
(22) Kittrell, J. *Adv. Chem.* **1970**, *8*, 97.
(23) Froment, G.; Bischoff, K. *Chemical Reactor Analysis and Design*, 2nd ed.; John-Wiley & Sons: New York, 1990.

p-nitrophenol concentration on the initial hydrogenation rate was investigated at different temperatures. The analysis of initial rate data showed that the gas−liquid, liquid−solid, and intraparticle mass-transfer resistances were not significant. A kinetic model based on Langmuir−Hinshelwood mechanism was found to represent the hydrogen kinetics well. The apparent energy of activation was found to be 61 kJ/mol.

NOTATION

a_B	effective gas−liquid interfacial area, m^2/m^3
a_P	effective liquid−solid interfacial area per unit volume of slurry, m^2/m^3
A,A^*	dissolved concentration of hydrogen, $kmol/m^3$
B	liquid-phase concentration of *p*-nitrophenol, $kmol/m^3$
d_P	particle diameter, m
D_{eA}	effective diffusivity of hydrogen in liquid phase, m^2/s
H	Henry's constant for hydrogen in ethanol, $kmol/m^3 \cdot MPa$
k_1	kinetic constant, $(m^3/kg)(m^3/kmol \cdot s)$
k_L	gas−liquid mass-transfer coefficient, m/s
k_s	liquid−solid mass-transfer coefficient, m/s
K_A	adsorption equilibrium constant for hydrogen, $m^3/kmol$
K_B	adsorption equilibrium constant for *p*-nitrophenol, $m^3/kmol$
N	average catalytic activity, kmol/kg·hr
r_{exp}	observed rate of hydrogenation, $kmol/m^3 \cdot s$
r_{mod}	predicted rate of hydrogenation, $kmol/m^3 \cdot s$
R_A	rate of hydrogenation, $kmol/m^3 \cdot s$
w	catalyst loading, kg/m^3

Greek Letters

ϵ	dielectric constant
ρ_p	particle density, kg/m^3

Acknowledgment

M.J.V. and S.M.K. thank the Council of Scientific and Industrial Research (CSIR), New Delhi, India for the award of Senior Research Fellowship.

Received for review September 6, 2002.

OP025589W